

University of Alberta
Department of Civil Engineering



Structural Engineering Report No. 97

**Full-Scale Test
of
A Composite Truss**

by
Reidar Bjorhovde

June, 1981

Structural Engineering Report No. 97

FULL-SCALE TEST
OF
A COMPOSITE TRUSS

by

Reidar Bjorhovde

Department of Civil Engineering

University of Alberta

Edmonton, Alberta, Canada

June, 1981

ABSTRACT

The report presents the evaluation of the design and full-scale testing of a composite (steel-concrete) truss. The span of the truss was 12 m (40 ft), and it was 0.85 m (2.8 ft) high, with a 63 mm (2½ in) normal weight concrete slab on a 76 mm (3 in) corrugated steel deck.

The test showed elastic response of the truss in the service load range. Midspan deflection to span ratio at service load was 1/524. The test ultimate load exceeded the design value by 7%.

Overall failure was precipitated by the buckling of a compression diagonal of the truss. The report details the failure and why this particular mode prevailed, and makes recommendations with regard to design and construction procedures.

LIST OF FIGURES AND PHOTOGRAPHS

	<u>Page</u>
Figure 1 Overall Truss Configuration and Instrumentation	23
Figure 2 Cross Section of Truss	24
Figure 3 Load Application Points and Support Conditions	25
Figure 4 Load-Deflection Curve for Truss	26
Figure 5 Load-Deflection Curve for Truss	27
Photograph 1 Overall Test Setup	28
Photograph 2 Close-up View of 120 kip Jack at Load Application Point	29
Photograph 3 Measurement of Deflections with LVDT's	30
Photograph 4 Detail of Strain-Gage Attachment at Top Chord Panel Point k	31
Photograph 5 Close-up Views from Different Angles of the Point and Member where Failure was Initiated	32
Photograph 6 Close-up of Underside of Steel Deck after Truss Failure, Showing Bulge in Wall of Deck where a Shear Stud had been Placed Very Close	33
Photograph 7 Appearance of Top of Concrete Slab after Truss Failure, Indicating Transverse and Longitudinal Cracking	33

TABLE OF CONTENTS

	<u>Page</u>
Abstract	ii
List of Figures and Photographs	iii
Table of Contents	iv
1. INTRODUCTION	1
2. DESCRIPTION OF COMPOSITE TRUSS	3
3. TESTING PLAN	6
4. TEST RESULTS	7
4.1 Material Properties of Steel and Concrete	7
4.2 Composite Truss	9
5. DISCUSSION OF FULL-SCALE TEST RESULTS	13
6. SUMMARY AND CONCLUSIONS	17
7. BIBLIOGRAPHY	20
8. ACKNOWLEDGEMENTS	21
9. FIGURES AND PHOTOGRAPHS	22
APPENDIX: LVDT AND STRAIN GAGE READINGS.	34

1. INTRODUCTION

The study of a full-scale composite truss that is presented in this report was conducted in the late summer and fall of 1979. It was undertaken at the request of two of the contractors for the Principal Plaza building, which is a 31-story steel-framed structure, located on Jasper Avenue in downtown Edmonton, Alberta, Canada.

Research on the behavior and strength of composite trusses has been very limited, and a literature review indicated that such topics had been addressed mostly in the context of composite joists. Although a steel joist is nothing but a truss, its design criteria come from the steel joist standards, and the method of fabrication is automated as much as feasible. Thus, resistance welds are commonplace with many of the steel joists that are in use today. Furthermore, the many types of joists that are commercially available are different in many respects, and reflect the preferences and methods of fabrication of the individual producers.

The common open-web steel joist is typically a very flexible member. This, together with its mass-produced nature, is the one criterion that sets it apart from the structural truss. The latter has been analyzed and designed by the structural engineer for the project, including detailed checks of member and connection capacities, as well as stiffness (i.e. deflection) properties. In the case of the composite truss, further analyses also have been made of shear connectors, concrete slab, and the interaction between the steel truss and the slab.

The lack of extensive and detailed research on composite trusses essentially forces the structural designer to rely on code

requirements that have been developed on the basis of and for composite beams. The latter utilize rolled or welded steel wide-flange beams (typically), on top of which is placed the concrete slabs. Whereas the basic concepts of analysis should hold true whether the steel portion of the composite member is solid or not, the differences between the truss and a wide-flange beam are such that additional concerns might be addressed. Some of these problems are itemized below, but it must be emphasized that the list does not pretend to be an exhaustive enumeration of all unresolved composite truss questions.

- (i) Concrete slab stresses in a composite truss.
- (ii) Shear transfer between slab and truss, particularly with respect to the top chord and how the loads are distributed from the top chord to the rest of the truss.
- (iii) Design of shear connectors.
- (iv) Local stress concentrations in the truss, particularly at panel points in the top chord, and around shear connectors.
- (v) Deflection analysis of the composite truss, both with respect to shoring requirements, live load deflection criteria, long term effects, and partial composite action.
- (vi) Stability of the bare steel truss during erection.

Some of the above questions prompted the study of the Principal Plaza truss in the first place, but the purpose of the full scale test was to determine whether the truss behaved satisfactorily and had adequate strength and stiffness to carry the design ultimate and service loads. Any further research will come as an outgrowth of this limited goal-oriented project.

2. DESCRIPTION OF COMPOSITE TRUSS

Figures 1 and 2 (Chapter 7 of the report contains all figures and photographs) illustrate the overall dimensions and cross-sectional details of the truss. It is noted that the span was 12 000 mm (40' - 0''), with panel points located at center-to-center spacings of 1000 mm (approximately 39.4''). The design as well as test end support conditions were simple, as indicated in Figure 3.

The cross-sectional sketch of the truss (Figure 2) also gives the details as regards truss and slab member sizes. This is given in detail below, including the material properties.

(a) Truss

Bottom Chord: HSS 76 x 127 x 6.4

Top Chord: HSS 76 x 100 x 6.4

All Diagonals: 2-L 75 x 75 x 4.8

All Verticals: HSS 76 x 76 x 3.2

The steel grade for the HSS members was CSA G40.21, 55W, with $F_y = 55$ ksi (380 MPa) and subsequent tension test results showed that these shapes were of production Class C. The steel grade for the angles that were used as diagonals throughout had a yield stress of $F_y = 50$ ksi (350 MPa).

(b) Concrete Slab

Normal weight (145 pcf; 2300 kg/m³) concrete with a specified strength of 25 MPa (3600 psi) was used for the slab, with a thickness of 63 mm (2½ inches) above the top of the ribs of the corrugated steel deck (see Figure 2). The concrete was delivered by a local ready-mixed concrete company, and poured and cured in the laboratory where the test was to be performed.

(c) Steel Deck

76 mm (3 in.) Westeel-Rosco high-bond corrugated steel deck was used. The ribs of the deck were placed perpendicular to the longitudinal axis of the truss. The Westeel-Rosco designation for the deck was T-30V, but a few panels of cellular deck (Westeel-Rosco type T-30-8F) were used in two areas of the span of the truss, to duplicate the actual building conditions.

The steel deck thickness was 1.22 mm (0.048 inches), exclusive of the galvanizing that also was used for the deck in the actual structure.

(d) Stud Shear Connectors

As indicated in Figure 2, 20 mm (3/4 inch) diameter headed stud shear connectors of 115 mm (4½ inches) length were used to provide the requisite shear connection between the truss and the slab. The studs were to be placed in the center of the deck corrugations, and a total of 22 such studs were placed evenly along the length of the top chord. The shear connectors were welded to the truss before the deck was placed, due to insufficient electrical power in the laboratory. This differed from the practice on the construction site, where the deck was placed first, and the studs then welded directly through the deck. However, both methods are acceptable, and do not influence the strength and behavior of the member as a whole.

As it will be shown later, it was discovered that certain studs had been located somewhat away from their intended point of

application. This caused them to come quite close to the wall of the deck corrugation, and it appears to have been the initiator of the failure of the truss. Further details will be given in Chapter 5.

Reinforcement in the concrete slab was identical to that used in the actual structure, namely, 150 x 150 - P9/P9 (6 x 6 - 10/10) welded wire mesh. No other reinforcing bars were utilized.

The original design of the structure called for a bare truss camber of 30 mm (1.18 in.). When the truss had been placed on the test supports, measurements showed that the camber was very close to the called-for value. The camber remaining after the slab had been cast (unshored construction) was 15.5 mm (0.61 in.).

3. TESTING PLAN

The specified properties of the materials have been indicated in Chapter 2. However, in accordance with good experimental practice it was decided to perform concrete and steel materials properties tests. These included two concrete cylinder tests at each of the ages 7, 14, 21 and 28 days, as well as tension tests from two verticals, four diagonals, and the bottom chord (2 tests) of the truss. Unfortunately, the material from the top chord could not be tested.

The truss itself would be tested as shown in Figure 3, using simply supported ends and three equal loads applied at the quarter points. 535 kN (120 kip) hydraulic actuators were placed at the load points, and all three were controlled from the same source. Photographs 1 and 2 illustrate the overall test setup in the laboratory, and a close-up view of the actuator (jack).

The truss was instrumented as shown in Figure 1. A total number of 18 strain gages (placed in 9 pairs) were applied to the truss and the steel deck as indicated. In addition, vertical deflections were measured at five locations, using LVDT's (linearly variable displacement transducers). The entire instrumentation and load control system was monitored by the Nova 2/10 computer of the Structural Engineering Laboratory.

Of particular interest were the strain measurements at the center and towards the ends of the top chord, as well as the deflection data from the LVDT that was located at midspan.

Photographs 3 and 4 illustrate some details of the instrumentation that was used.

4. TEST RESULTS

4.1 Material Properties of Steel and Concrete

The compressive strength data for the concrete at ages 7, 14, 21 and 28 days are shown in Table 1. Each strength given represents the average of two cylinder tests. Noting that the minimum specified concrete strength was 25 MPa (3600 psi), it is seen that the concrete was approximately 10 percent stronger than required. This type of variation is, of course, taken into account in the design procedure through the value of the performance factor. It is observed that the truss had been designed on the basis of limit states principles, using the requirements of CSA Standard S16.1-M78.

TABLE 1
Compressive Strengths of Concrete

Nos.	Age (days)	Strength (MPa)	Strength (psi)
1,2	7	17.2	2499
3,4	14	22.5	3263
5,6	21	25.6	3716
7,8	28	27.9	4051

Dynamic yield stress values and ultimate elongations of the steel are shown in Table 2. These data were obtained from tension specimen tests on full-thickness coupons, made and tested in accordance with the requirements of ASTM Standard A370. In the case of the specimens that were taken from HSS members, the yield stress given in the table is the stress recorded for a permanent deformation of 0.2 percent, as

observed in the stress-strain diagram. For tension coupons cut from truss diagonals, the stress is that determined from the yield plateau.

It is seen that the minimum specified requirements have been met for all specimens, with the exception of the ultimate elongation that was recorded from specimens V₁, B₁, and B₂. Noting that the ultimate elongation was measured over a 50 mm (2 inch) gage length, the underrun cannot be characterized as serious, especially since the strength levels are more than adequate, and the structure is statically loaded. In Table 2 the specimen designations V, B and D refer to vertical, bottom chord and diagonal, respectively. The number following the letter identifies the specimen and its location.

TABLE 2
Material Properties of Steel

No.	Shape	Yield Stress (dynamic) (MPa)	(ksi)	Elongation % (50 mm gage length)
V1	HSS	531	77.1	10.7
V2	HSS	515	74.8	31.3
B1	HSS	476	69.1	7.2
B2	HSS	442	64.2	14.0
D1	Angle	362	52.5	22.0
D2	Angle	368	53.4	31.0
D3	Angle	350	50.7	23.0
D4	Angle	351	50.9	22.0

4.2 Composite Truss

Detailed measurement data, in the form of LVDT and strain gage readings for each load level of the composite truss test, are given in the Appendix of this report. Figure 1 shows the locations and orientations of the measuring equipment. Figures 4 and 5 give the load-deflection curve for the truss, where load per jack is plotted along the vertical axis, and midspan deflection is plotted along the horizontal axis.

A special note must be made with regard to the deflection readings. The bare truss camber was 30 mm (1.18 in.), and after the concrete slab had been poured and cured, the remaining midspan camber was 15.5 mm (0.61 in.). The deflection data that are given in Figs. 4 and 5 were made with reference to the position of the bottom chord after the slab was in place. The actual truss deflection at midspan, i.e. the amount of displacement below the hypothetical horizontal bottom chord, therefore must be calculated as

$$\Delta = \Delta' - 15.5 \quad (1a)$$

for a deflection in mm, and as

$$\Delta = \Delta' - 0.61 \quad (1b)$$

for a deflection in inches. Δ' indicates the deflection values given in Figs. 4 and 5, as well as in the Appendix.

Figure 4 and its explanatory notes describe the overall behavior characteristics of the truss during the test. The initial response was linearly elastic for all practical purposes, up to a load of 40 kN (9 kips) per load point, or a total load on the truss of 120 kN (27 kips). The end of the elastic region is indicated as point A on the load-deflection curve. The deflection measured at this stage was 15.1 mm (0.59 in.), giving a true midspan displacement of -0.4 mm (-0.02 in.), or, in other words, the bottom chord was very close to the horizontal.

Subsequent load increases produced an increasingly non-linear response of the truss, as evidenced by the load-deflection curve up to point I. The service load was reached at a load per jack of 80 kN (18 kips), (point B on the curve), at which time the total deflection was recorded as 38.4 mm (1.51 in.). The true deflection becomes 22.9 mm (0.90 in.). This corresponds to a deflection to span ratio of 1/524 for the true deflection; 1/313 for the total displacement.

As the load reached 102 kN (23 kips) per load point (point I in Fig. 4), diagonal F-k towards the southern end of the truss buckled (see Fig. 1 for the location of this member). This was preceded by significantly higher strain readings for strain gage no. 5 (see Fig. 1, and the Appendix). The reasons for this will be evaluated in Chapter 5 of this report. Suffice it to observe at this point, however, that subsequent examination of the failure region in the top chord and in the slab directly above panel point k revealed that the shear stud at this location had been placed off-center; too close to the wall of the corrugated steel deck. This forced the chord to carry a larger

share of the internal stress resultant at this point, producing early local yielding, and reducing the end restraint for the compression diagonal F-k.

Diagonal F-k buckled at a load slightly below the design ultimate load of 107 kN (24 kips) per load point. At this stage the load was reduced to 22 kN (5 kips) per jack, and the double angle diagonal was reinforced with a plate. The plate was welded to both angles after they had been somewhat straightened, as can be seen in Photographs 5(a), (b) and (c).

Upon re-application of the load, the response of the truss was essentially linearly elastic, up to a load per jack of 93 kN (31 kips). This can be seen from the load-deflection curve in Fig. 4, between points II and III. The subsequent load increments were purposely made very small, as the deflection readings gave evidence of rapidly approaching maximum load. Point III in Fig. 4 indicates that the maximum load of the truss was reached at 114 kN (25.5 kips) per jack, or for a total load of 342 kN (76.5 kips). The total deflection at midspan was 84.8 mm (3.34 in.), with a true deflection of 69.3 mm (2.73 in.). At this stage the diagonal F-k buckled again, accompanied by tearing of the welds that attached the angles of the diagonal to the HSS top chord. The shape of the buckled diagonal can be seen in Photographs 5, as can the torn weld (Photographs 5(b) and (c)).

The failure took place at a load slightly above the design ultimate value of 107 kN (24 kips) per load point. The load ratio is

$$LR = \frac{\text{Actual ultimate load}}{\text{Design ultimate load}} = \frac{114}{107} = 1.07$$

In other words, the truss withstood a load 7 percent above that predicted by the design ultimate analysis.

Examination of the structure after the completion of the test showed very little distress in the stud shear connectors, including the one located directly above panel point k. However, the influence of misplaced shear studs can be discerned also from Photograph 6, where a bulge is visible in the wall of a corrugation of the steel deck. Similar large distortions were found in all locations where studs had not been accurately placed.

Photograph 7 illustrates the appearance of the top surface of the concrete slab, directly above panel point k. The failure of the connection between the slab and the truss at this point prompted a loss of composite action. This, in turn, produced a higher stress resultant in the slab (compression in the longitudinal direction), which prompted a tensile failure in the concrete through Poisson's effect. This is shown as the longitudinal crack in Photograph 7.

The loss of composite action also introduced a higher bending moment in the slab at the panel point. With tensile strains being developed in the surface of the slab, transverse cracks also developed. These can be seen in Photograph 7 as well.

5. DISCUSSION OF FULL-SCALE TEST RESULTS

The composite truss was designed on the basis of the composite member criteria of CSA Standard S16.1-M78 (1). These are ultimate strength based, and were developed from analyses and tests of "normal" composite members. That is, the rules were formulated for beams with solid slabs and hot-rolled or welded built-up wide-flange shapes. This is particularly important to bear in mind when the results are evaluated, and comparisons are made with existing design approaches.

The truss was analyzed as a two-dimensional structure, using the properties of the bottom chord, the diagonals, and the verticals as given in the Canadian Institute of Steel Construction "Handbook" (2). The properties of the top chord were computed on the basis of the properties of the HSS 76 x 100 x 6.4 (see Fig. 2) and the transformed area of the effective concrete slab. It is noted that the governing effective width of 2300 mm was determined as required by the design standard. However, its validity is presently being scrutinized by researchers, especially whether it is applicable to deeper composite members (3). It is also relevant to observe that the method of slab area transformation strictly is based on elastic principles, assuming that the slab and the steel both are fully effective, and that plane sections remain plane (4). The effects of less than 100% composite action, slip between the slab and the steel, and material and structural behavior as the ultimate load is being reached, are not well understood. For the purposes of this evaluation, therefore, it is assumed that strain compatibility applies. Transformation of the concrete slab into an equivalent steel area then is achieved through the normal procedure of

dividing A_c , the area of concrete, by the modular ratio, $n = E_s/E_c$, where E_s and E_c are the moduli of elasticity for steel and concrete, respectively. For this case, $n = 11.7$.

Because the steel deck corrugations were oriented perpendicularly to the longitudinal axis of the truss, only the concrete slab above the top of the corrugations was considered effective. This is the commonly used procedure for hollow-core floor systems (5,6). However, it is noted that the effective width is computed on the basis of the combined thickness of the deck and the slab (139 mm in this case).

The actual sizing of the components of the truss is typically based on a "first principles" approach to composite design (7), whereby equilibrium in the cross section at ultimate load is assured. Thus, the stress in the concrete at this stage is rectangularly distributed with an intensity of $0.85 f'_c$ and the steel top and bottom chords will both have reached yield. The web members of the truss are not considered in this analysis. This is a conservative assumption.

With a combined dead load of the steel truss and the 2300 mm wide slab of approximately 6800 kg (15,000 lbs), the design called for a service load of 80 kN (18 kips) per load point, above and beyond the dead load. Deflection analysis was linearly elastic. As can be seen from Fig. 5, although some non-linearity between load and deflection was evident by the time the service load was reached (point B in Fig. 4, Load No. 11 in Fig. 5), the subsequent unload-reload cycle displayed elastic response of the truss. It is therefore sufficiently accurate to base all service load level calculations on elastic properties.

As observed in Chapter 4, the true service load deflection at midspan was 22.9 mm (0.90 in), giving a deflection to span ratio of 1/524. This is well below the commonly accepted ratio of 1/360, which applies to the allowable deflection under service load. The composite truss therefore was very stiff, as expected.

The studs that had been mis-located on the top chord were the cause of the initial failure of the truss, as observed in Chapter 4. This is particularly critical in the area around panel point k (see Fig. 1), since the internal stress resultants in the slab and the chord and diagonal members were high. (It is noted that the studs were not out of place at the north end of the truss, which is symmetrical to the southern half with respect to midspan.)

The mechanism of the failure has already been explained. The reason that such a seemingly insignificant error as the mis-placement of a stud could precipitate the overall failure must be sought in the relative sizes of the slab and the truss members. The cross-sectional area of the HSS 76 x 100 x 6.4 top chord is 1990 mm² and its moment of inertia about the horizontal axis (see Fig. 2) is $2.68 \cdot 10^6$ mm⁴. The wall thickness of the HSS is 6.4 mm. The misplacement of the stud caused a premature loss of composite action in the vicinity of panel point k. This, combined with the relatively small steel area, made the joint more sensitive to small changes in internal stress resultants. This became compounded as local yielding developed.

The problem might not have been as prevalent if the slab reinforcement had been larger. As has been demonstrated in research on stub-girder floor systems (3,8), the amount of longitudinal as well as transverse slab reinforcement is important to the overall ductility and performance of the flexural member. In the case of the composite truss, only welded wire mesh 150 x 150 - P9/P9 was used. On a strict strength calculation basis, this would be adequate, but for overall performance it would be advantageous to incorporate additional steel.

The above observation is further emphasized by the pattern of slab cracks that developed. Additional transverse reinforcement would have helped delay the development of the longitudinal crack (see Photograph 7). Similarly, more longitudinal reinforcing steel would have increased the axial load and bending moment capacity of the slab, causing a retention of composite action to higher loads. In addition, this reinforcement would also make more of the slab more efficient in its load-sharing with the steel truss.

The ultimate load calculation turned out to be reasonably accurate, in that the truss failed at a load only 7% above the design ultimate load. There is therefore no doubt that the truss performed adequately both at the service as well as the ultimate load level. However, barring the premature failure of one of the members, it is believed that the truss would have been able to sustain an ultimate load well above the one that was found. This is somewhat speculative at this stage; only additional research can substantiate the observation.

On the whole, therefore, it can be stated that the design and performance of the structure were adequate at all load levels.

6. SUMMARY AND CONCLUSIONS

This report has presented a description and evaluation of the design and full-scale test of a composite truss, identical to those used in the Principal Plaza building in Edmonton, Alberta, Canada. The truss configuration and materials have been detailed, as have the testing procedure and equipment. The analysis of the test results and a comparison with the design data lead to the following conclusions:

1. The truss had been designed on the basis of the limit states design principles of the Canadian Standard S16.1-M78. Although these criteria were developed for very different composite members, the structure performed adequately as far as the design conditions are concerned.
2. The response of the truss up to the computed service load level was elastic for all practical purposes. The true midspan service load deflection was 22.9 mm (0.9 in), which gives a deflection to span ratio of 1/524 for the 12,000 mm span. The truss therefore was very stiff in the service load range.
3. The total failure load of the truss was 342 kN (76.5 kips) (114 kN (25.5 kips) per load point). This compares to the design ultimate load of 321 kN (72 kips), giving a ratio of true ultimate load to design ultimate load of 1.07. In other words, the structure exceeded the design capacity by 7%. The true deflection at ultimate load was 69.3 mm (2.73 in).
4. At a load equal to 95% of the design ultimate value, one of the compression diagonals towards the southern end of the truss buckled. This was found to have been prompted by a mis-located

shear stud directly above the panel point in the top chord where the diagonal ended. This caused a premature loss of composite action at this point, with the result that the slab and the truss chord both had to carry a higher load than anticipated.

5. Unloading, repair and reloading of the truss brought it to its actual ultimate load of 342 kN (76.5 kips). The failure was caused by the buckling of the same diagonal that failed earlier. The truss response was linearly elastic for a large range of the reloading cycle.
6. Service load design can be based on elastic properties. The correlation between design and actual behavior was very good.
7. Until the current questions regarding the design of deep composite members have been resolved, it appears satisfactory to continue using the accepted ultimate strength principles.
8. The concrete slab had only a minimal amount of longitudinal and transverse reinforcing steel (150 x 150 - P9/P9 (6 x 6 - 10/10) welded wire mesh). The mode of failure in the slab was a combination of a longitudinal crack directly above the truss chord, and transverse slab cracks. It is believed that additional reinforcement would have helped the truss to carry a higher ultimate load, in particular by giving the slab more strength and ductility.
9. The shear connection between the slab and the top chord of the truss appeared satisfactory, judging from post-test examinations of the studs and the slab and truss chord in the vicinity

of the studs. No studs gave any indication of having been overstressed.

10. The accurate placement of stud shear connectors is important in hollow core floor systems. In particular, studs should not be placed too close to the walls of the corrugations of the steel deck. However, it is noted that the service load performance of the truss was not affected by this condition.

7. BIBLIOGRAPHY

1. "Steel Structures for Buildings - Limit States Design", Canadian Standards Association, Standard No. S16.1-M78, Rexdale, Ontario, 1978.
2. "Metric Structural Steel Design Data", Canadian Institute of Steel Construction, Willowdale, Ontario, November, 1978.
3. Zimmerman, T.J.E., and Bjorhovde, Reidar, "Analysis and Design of Stub-Girders", Structural Engineering Report No. 90, University of Alberta, March, 1981.
4. Tall, Lambert, Editor-in-Chief, "Structural Steel Design", 2nd Edition, Ronald Press Company, New York, 1974.
5. Grant, J.A., Fisher, J.W. and Slutter, R.G., "Composite Beams with Formed Steel Deck", AISC Engineering Journal, Vol. 14, No. 1, First Quarter, 1977.
6. "Specification for the Design, Fabrication, and Erection of Structural Steel for Buildings", American Institute of Steel Construction, Chicago, Illinois, November, 1978.
7. Adams, P.F., Krentz, H.A., and Kulak, G.L., "Limit States Design in Structural Steel - SI Units", Canadian Institute of Steel Construction, Willowdale, Ontario, 1978.
8. Bjorhovde, Reidar, "Testing of Full-Size Stub-Girder", Report submitted to Dominion Bridge Company, Calgary, Alberta, June, 1981.

8. ACKNOWLEDGEMENTS

The author would like to express his appreciation to a number of individuals that were involved in the running of this project. Particular thanks are due Thor Gaul, then of C.W. Carry, Ltd., and Eric Jokinen, then of Read-Jones-Christoffersen, Ltd., for their work in procuring test specimens, drawings, and the like. C.W. Carry, Ltd., donated the materials and fabrication costs; Westeel-Rosco, Ltd., provided the steel deck.

Terry Sexton and Tom Zimmerman spent a great deal of time in the laboratory, both during the setup of the test specimen and its instrumentation, as well as during the testing itself. Naturally, the work of Chief Technician Larry Burden was crucial, especially since the testing took place during a period when the laboratory manpower was severely reduced. Last, but not least, Doreen Wyman did an outstanding job in typing the report.

9. FIGURES AND PHOTOGRAPHS

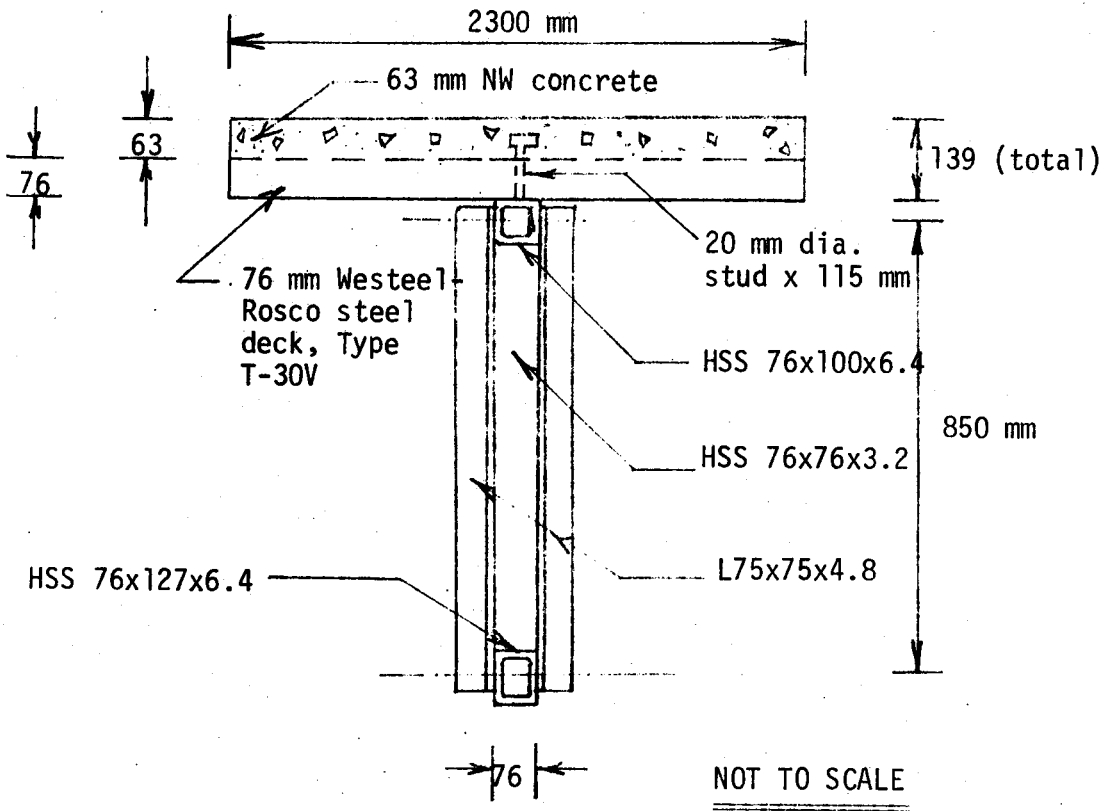


Fig. 2 Cross Section of Truss

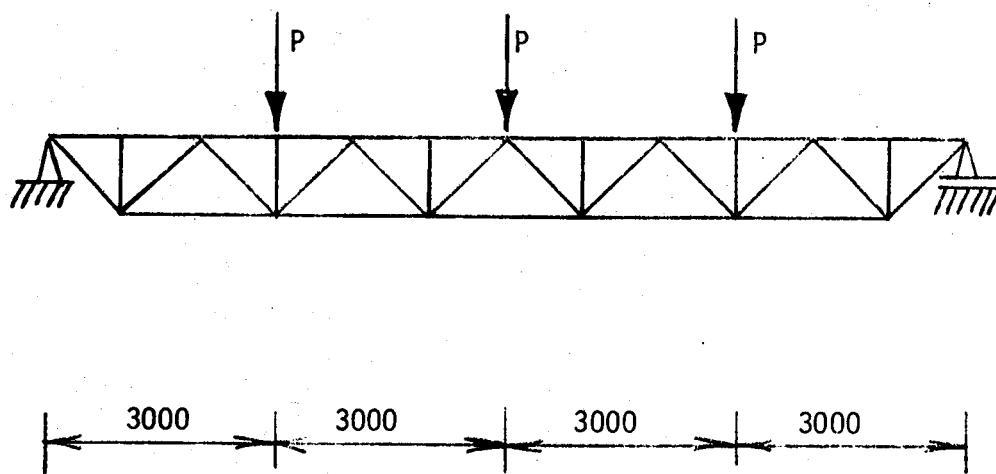


Fig. 3 Load Application Points
and Support Conditions

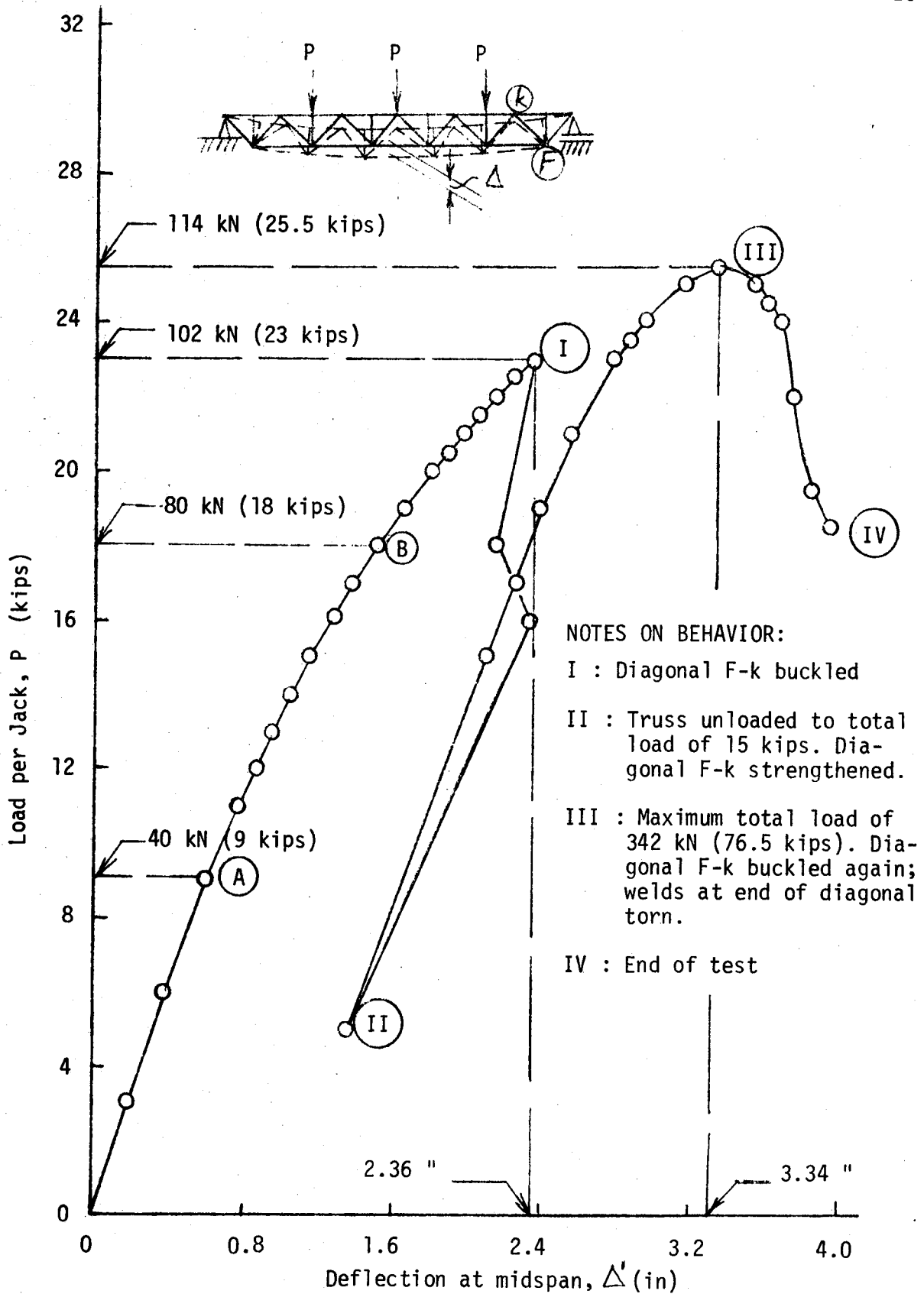


Fig. 4 Load-Deflection Diagram for Truss

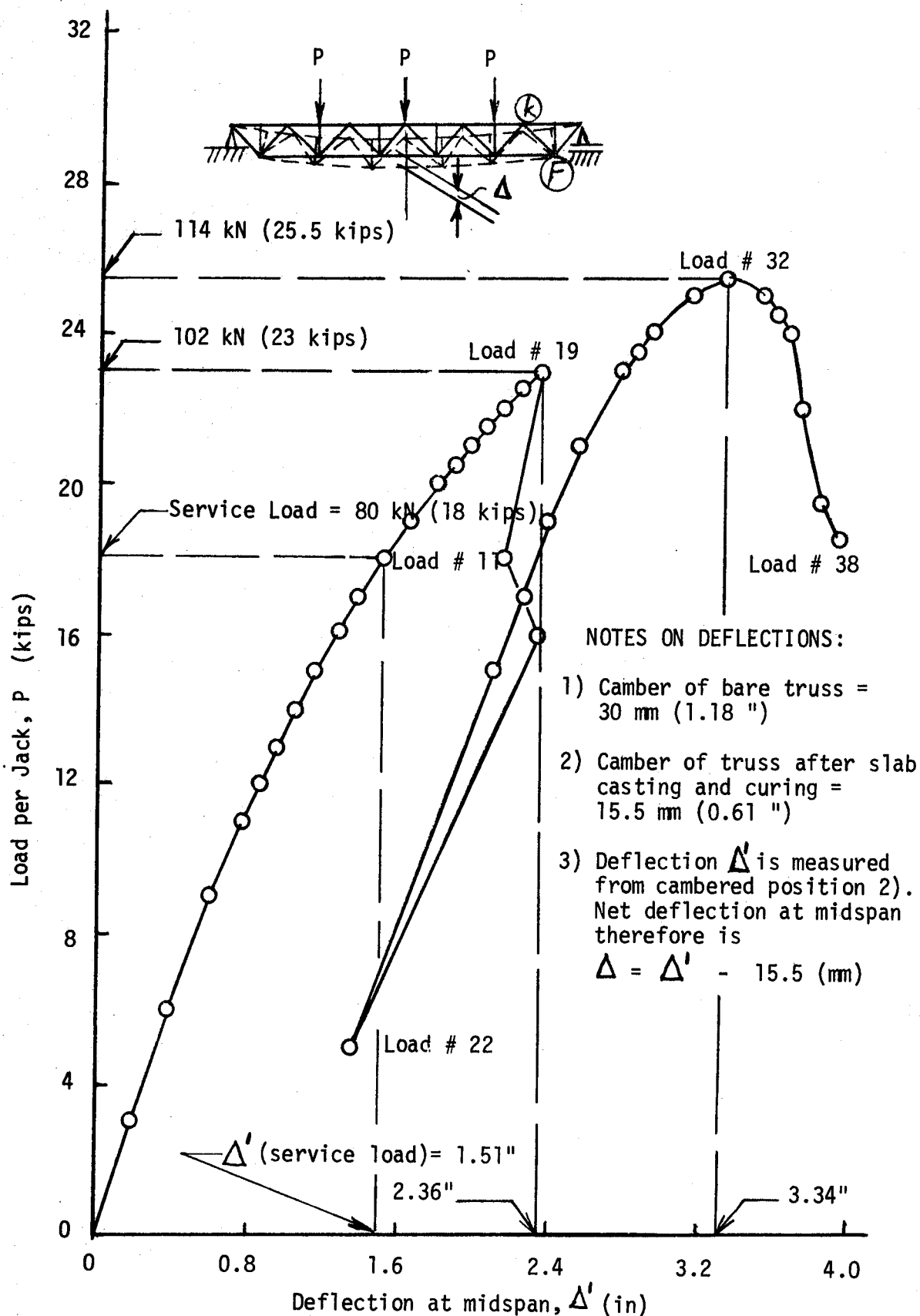
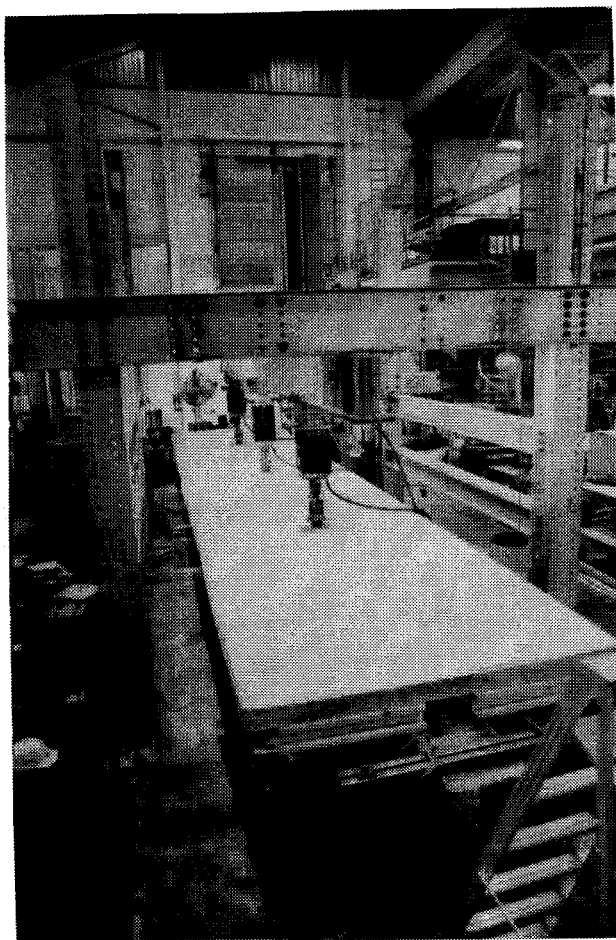
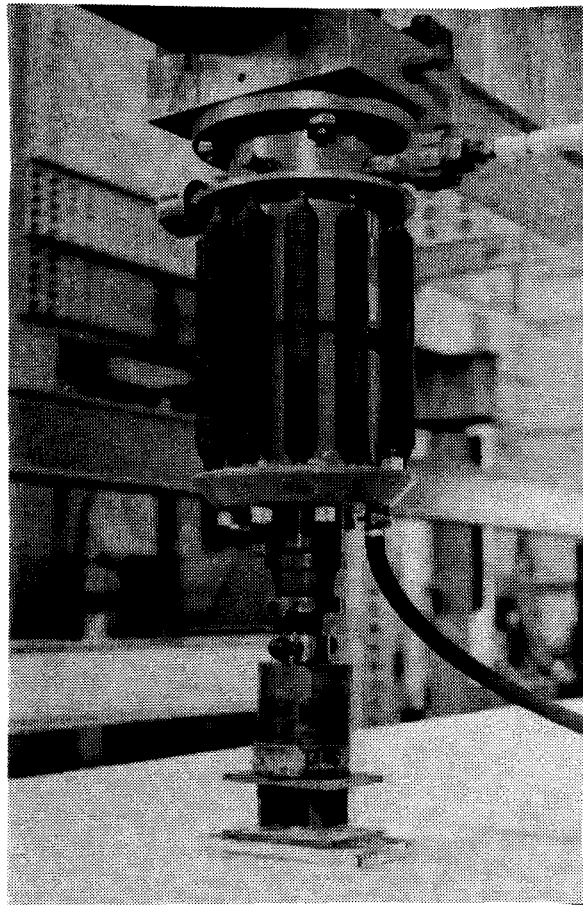


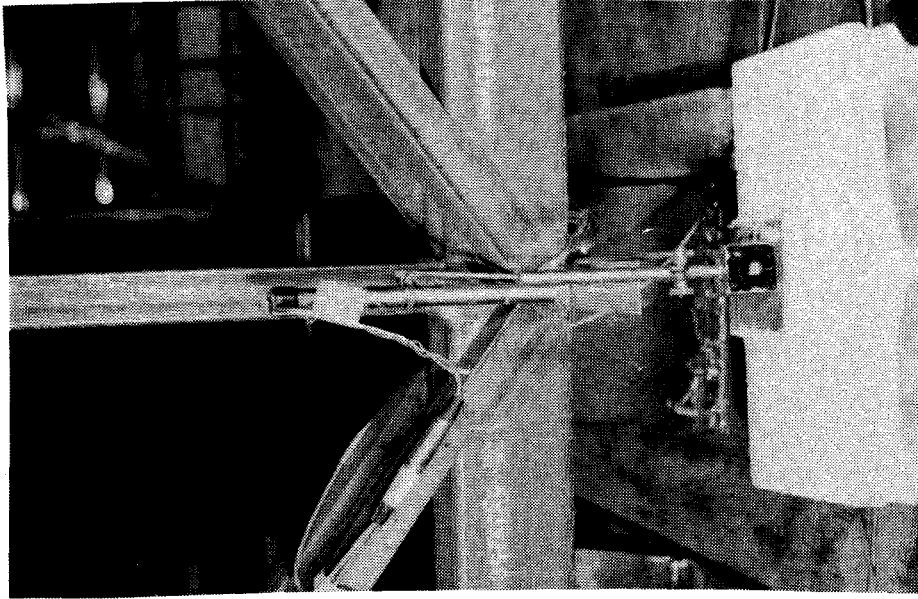
Fig. 5 Load-Deflection Diagram for Truss



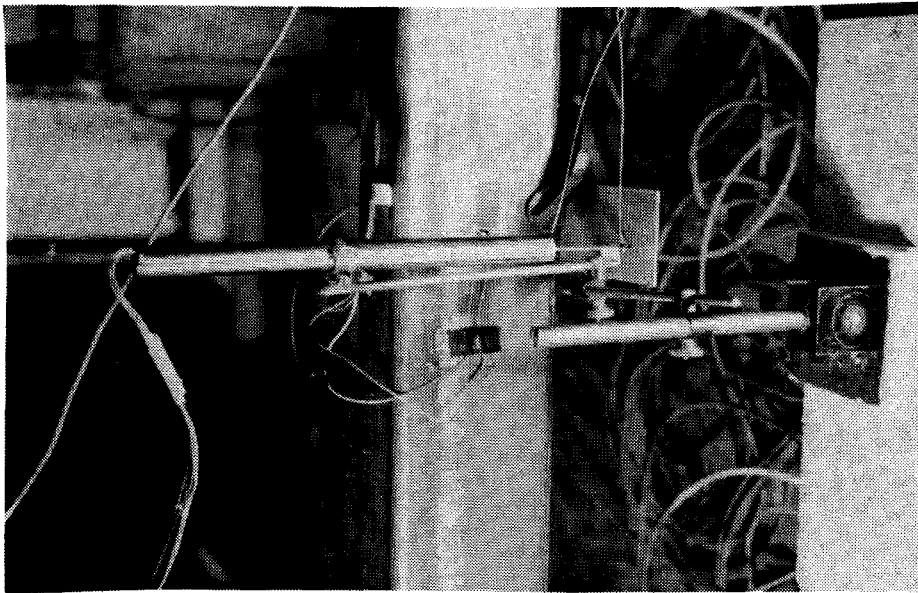
Photograph 1 Overall test setup



Photograph 2 Close-up view of 120 kip jack at load application point

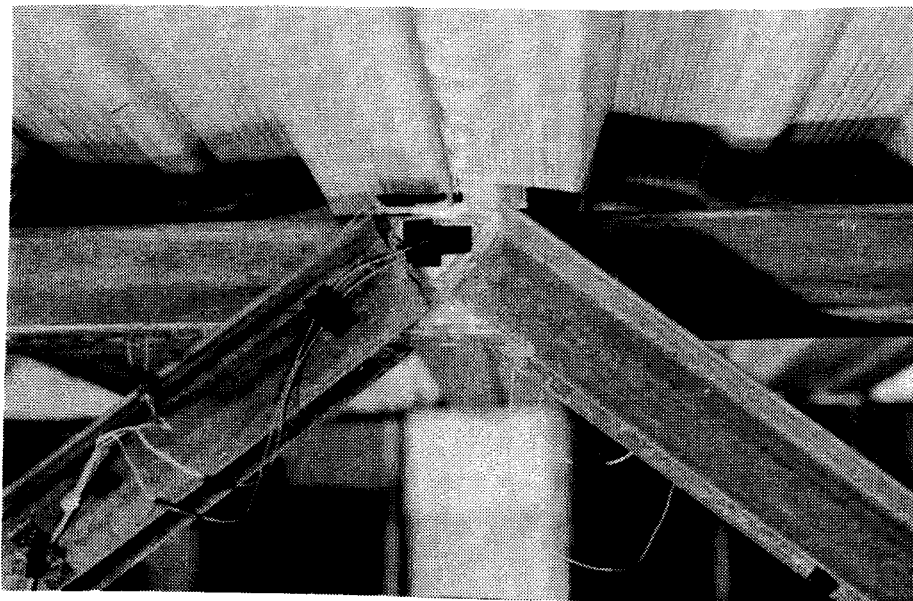


(b) Close-up at bottom chord quarter point

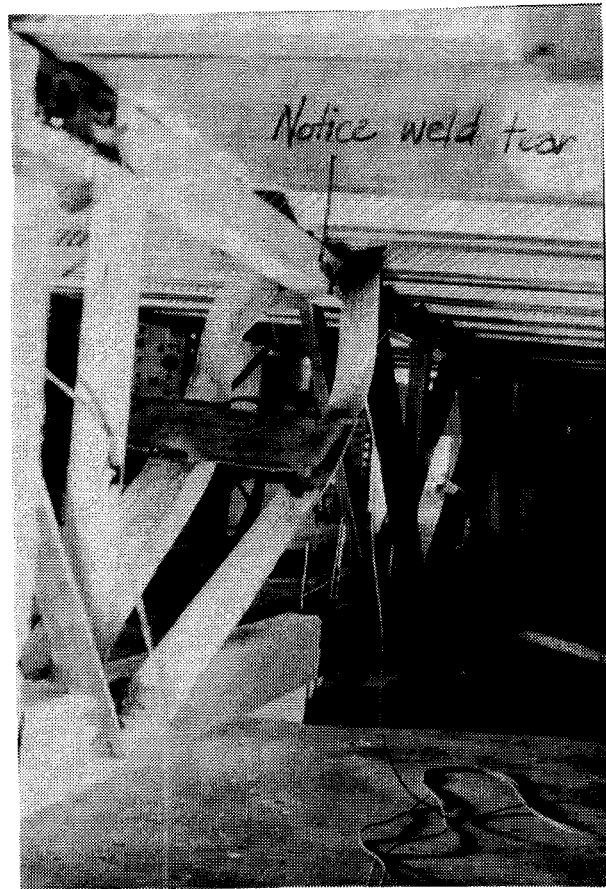
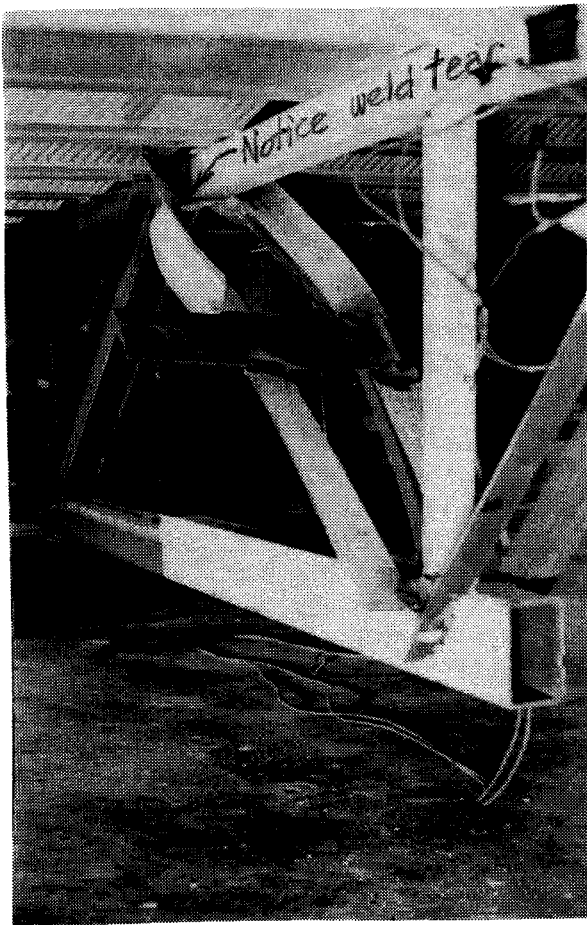
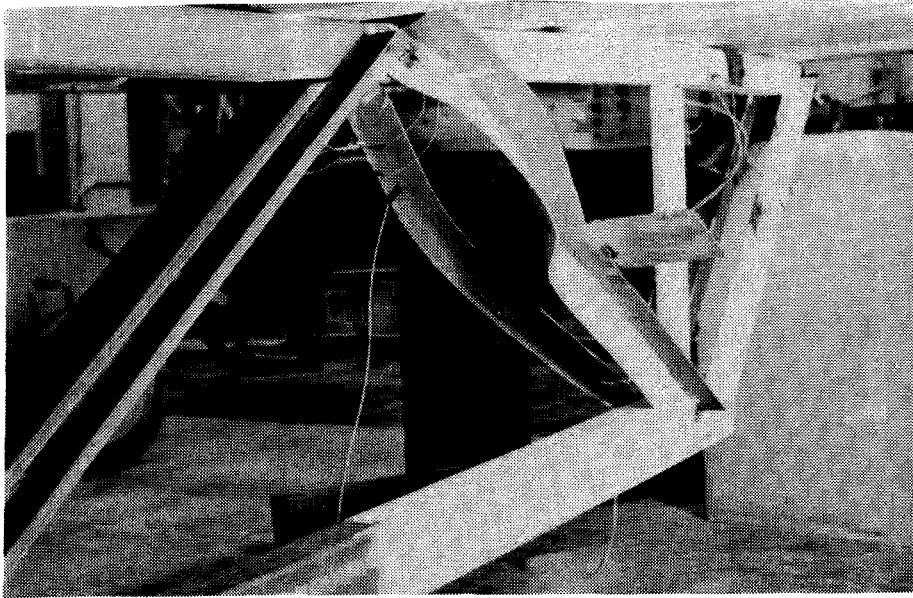


(a) Close-up at midspan

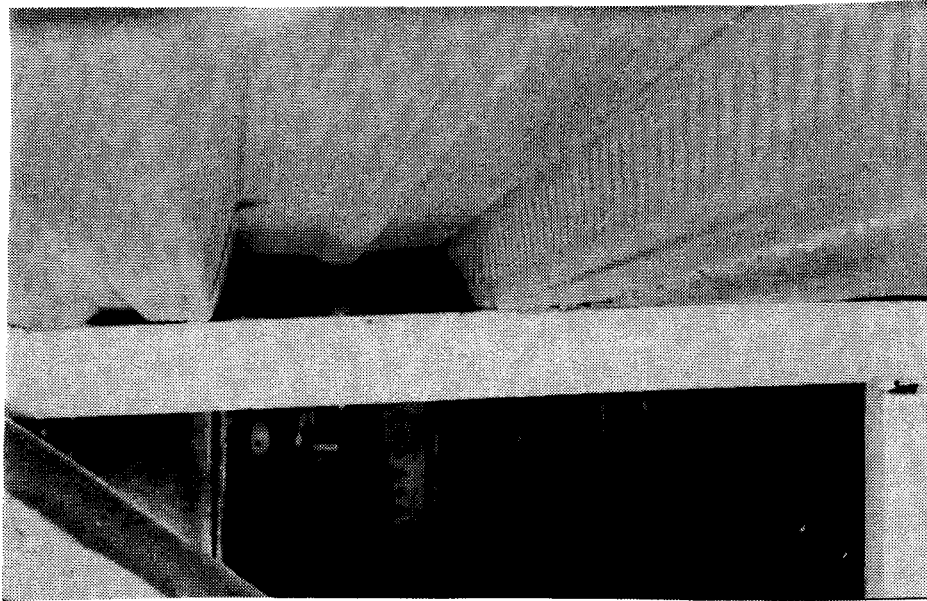
Photograph 3 Measurement of deflections with LVDT's



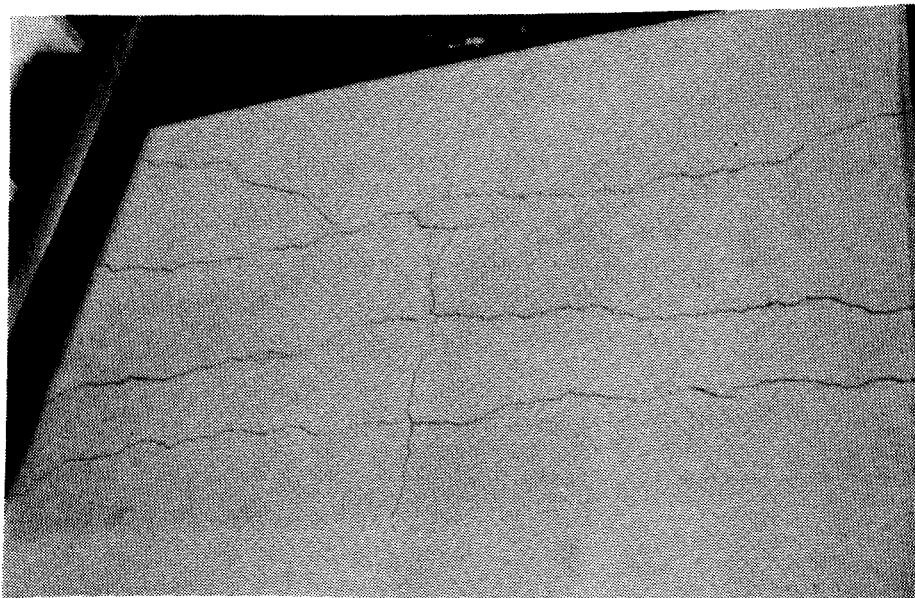
Photograph 4 Detail of strain gage attachment at top chord panel point k



Photograph 5 (a), (b), and (c) Close-up views from different angles of the point and member where failure was initiated



Photograph 6 Close-up of underside of steel deck after truss failure, showing bulge in wall of deck where a shear stud had been placed very close



Photograph 7 Appearance of top of concrete slab after truss failure, indicating transverse and longitudinal cracking

APPENDIX:

LVDT AND STRAIN GAGE

READINGS

VERTICAL REFLECTIONS (in) BOTTOM CHORD

LOAD #	LOAD (CLIPS) CHANNEL	Panel point 2		Panel point 3		Midspan 4		Panel point 5		Panel point 6	
		8	23	79	Panel point 2	Panel point 3	Panel point 4	Panel point 5	Panel point 6	Panel point 5	Panel point 6
0	0.0000E 0	0.0000E 0	0.0000E 0	0.0000E 0	0.0000E 0	0.0000E 0	0.0000E 0	0.0000E 0	0.0000E 0	0.0000E 0	0.0000E 0
1	0.3000E 1	0.1057E 0	0.01730E 0	0.1730E 0	0.1730E 0	0.1870E 0	0.1870E 0	0.1616E 0	0.1616E 0	0.3014E -1	
2	0.6000E 1	0.2358E 0	0.03476E 0	0.3476E 0	0.3476E 0	0.3792E 0	0.3792E 0	0.3278E 0	0.3278E 0	0.2087E 0	
3	0.9000E 1	0.3911E 0	0.05519E 0	0.5519E 0	0.5519E 0	0.5938E 0	0.5938E 0	0.5176E 0	0.5176E 0	0.3672E 0	
4	0.1100E 2	0.5090E 0	0.07158E 0	0.7158E 0	0.7158E 0	0.7652E 0	0.7652E 0	0.6729E 0	0.6729E 0	0.4827E 0	
5	0.1200E 2	0.5723E 0	0.08043E 0	0.8043E 0	0.8043E 0	0.8604E 0	0.8604E 0	0.7544E 0	0.7544E 0	0.5465E 0	
6	0.1300E 2	0.6332E 0	0.08900E 0	0.8900E 0	0.8900E 0	0.9519E 0	0.9519E 0	0.8336E 0	0.8336E 0	0.6103E 0	
7	0.1400E 2	0.6982E 0	0.09818E 0	0.9818E 0	0.9818E 0	0.1051E 1	0.1051E 1	0.9183E 0	0.9183E 0	0.6778E 0	
8	0.1500E 2	0.7628E 0	0.01073E 1	0.1073E 1	0.1073E 1	0.1146E 1	0.1146E 1	0.1005E 1	0.1005E 1	0.7446E 0	
9	0.1600E 2	0.8375E 0	0.01175E 1	0.1175E 1	0.1175E 1	0.1253E 1	0.1253E 1	0.1108E 1	0.1108E 1	0.8233E 0	
10	0.1700E 2	0.9197E 0	0.01289E 1	0.1289E 1	0.1289E 1	0.1376E 1	0.1376E 1	0.1223E 1	0.1223E 1	0.9115E 0	
11	0.1800E 2	0.1013E 1	0.01414E 1	0.1414E 1	0.1414E 1	0.1514E 1	0.1514E 1	0.1346E 1	0.1346E 1	0.1005E 1	
12	0.1900E 2	0.1105E 1	0.01540E 1	0.1540E 1	0.1540E 1	0.1657E 1	0.1657E 1	0.1477E 1	0.1477E 1	0.1111E 1	
13	0.2000E 2	0.1204E 1	0.01680E 1	0.1680E 1	0.1680E 1	0.1806E 1	0.1806E 1	0.1618E 1	0.1618E 1	0.1218E 1	
14	0.2050E 2	0.1266E 1	0.01770E 1	0.1770E 1	0.1770E 1	0.1901E 1	0.1901E 1	0.1710E 1	0.1710E 1	0.1289E 1	
15	0.2100E 2	0.1314E 1	0.01839E 1	0.1839E 1	0.1839E 1	0.1978E 1	0.1978E 1	0.1784E 1	0.1784E 1	0.1344E 1	
16	0.2150E 2	0.1373E 1	0.01919E 1	0.1919E 1	0.1919E 1	0.2063E 1	0.2063E 1	0.1864E 1	0.1864E 1	0.1407E 1	
17	0.2200E 2	0.1422E 1	0.01998E 1	0.1998E 1	0.1998E 1	0.2147E 1	0.2147E 1	0.1945E 1	0.1945E 1	0.1471E 1	
18	0.2250E 2	0.1485E 1	0.02088E 1	0.2088E 1	0.2088E 1	0.2243E 1	0.2243E 1	0.2038E 1	0.2038E 1	0.1548E 1	
19	0.2300E 2	0.1565E 1	0.02196E 1	0.2196E 1	0.2196E 1	0.2362E 1	0.2362E 1	0.2157E 1	0.2157E 1	0.1663E 1	
20	0.1800E 2	0.1408E 1	0.02008E 1	0.2008E 1	0.2008E 1	0.2177E 1	0.2177E 1	0.2007E 1	0.2007E 1	0.1607E 1	
21	0.1600E 2	0.1473E 1	0.02128E 1	0.2128E 1	0.2128E 1	0.2331E 1	0.2331E 1	0.2208E 1	0.2208E 1	0.1941E 1	
22	0.5000E 1	0.1134E 1	0.01219E 1	0.1219E 1	0.1219E 1	0.1357E 1	0.1357E 1	0.1282E 1	0.1282E 1	0.1137E 1	
23	0.1500E 2	0.1629E 1	0.01912E 1	0.1912E 1	0.1912E 1	0.2099E 1	0.2099E 1	0.1965E 1	0.1965E 1	0.1679E 1	
24	0.1700E 2	0.1733E 1	0.02059E 1	0.2059E 1	0.2059E 1	0.2253E 1	0.2253E 1	0.2109E 1	0.2109E 1	0.1794E 1	
25	0.1900E 2	0.1827E 1	0.02187E 1	0.2187E 1	0.2187E 1	0.2385E 1	0.2385E 1	0.2240E 1	0.2240E 1	0.1895E 1	
26	0.2100E 2	0.1937E 1	0.02344E 1	0.2344E 1	0.2344E 1	0.2552E 1	0.2552E 1	0.2401E 1	0.2401E 1	0.2020E 1	
27	0.2300E 2	0.2082E 1	0.02546E 1	0.2546E 1	0.2546E 1	0.2773E 1	0.2773E 1	0.2615E 1	0.2615E 1	0.2204E 1	
28	0.2350E 2	0.2134E 1	0.02623E 1	0.2623E 1	0.2623E 1	0.2857E 1	0.2857E 1	0.2698E 1	0.2698E 1	0.2276E 1	
29	0.2400E 2	0.2191E 1	0.02701E 1	0.2701E 1	0.2701E 1	0.2943E 1	0.2943E 1	0.2785E 1	0.2785E 1	0.2351E 1	
30	0.2450E 2	0.2252E 1	0.02799E 1	0.2799E 1	0.2799E 1	0.3046E 1	0.3046E 1	0.2893E 1	0.2893E 1	0.2439E 1	
31	0.2500E 2	0.2335E 1	0.02914E 1	0.2914E 1	0.2914E 1	0.3166E 1	0.3166E 1	0.3019E 1	0.3019E 1	0.2544E 1	
32	0.2550E 2	0.2447E 1	0.03080E 1	0.3080E 1	0.3080E 1	0.3343E 1	0.3343E 1	0.3203E 1	0.3203E 1	0.2725E 1	
33	0.1111E 5	0.2573E 1	0.03259E 1	0.3259E 1	0.3259E 1	0.3540E 1	0.3540E 1	0.3412E 1	0.3412E 1	0.2952E 1	
34	0.2450E 2	0.2595E 1	0.03312E 1	0.3312E 1	0.3312E 1	0.3607E 1	0.3607E 1	0.3500E 1	0.3500E 1	0.3086E 1	
35	0.2400E 2	0.2614E 1	0.03361E 1	0.3361E 1	0.3361E 1	0.3676E 1	0.3676E 1	0.3593E 1	0.3593E 1	0.3218E 1	
36	0.2200E 2	0.2630E 1	0.03397E 1	0.3397E 1	0.3397E 1	0.3741E 1	0.3741E 1	0.3699E 1	0.3699E 1	0.3443E 1	
37	0.1950E 2	0.2638E 1	0.03461E 1	0.3461E 1	0.3461E 1	0.3843E 1	0.3843E 1	0.3845E 1	0.3845E 1	0.3688E 1	
38	0.1850E 2	0.2679E 1	0.03539E 1	0.3539E 1	0.3539E 1	0.3941E 1	0.3941E 1	0.3964E 1	0.3964E 1	0.3865E 1	
39	0.0000E 0	0.1559E 1	0.01921E 1	0.1921E 1	0.1921E 1	0.2235E 1	0.2235E 1	0.2290E 1	0.2290E 1	0.2526E 1	

True Service Load

Diagonal
 (E) - (E)
 bus load

Max load

Test stop

STRAIN GAGE READINGS

Load No.	No. 1	No. 2	8	No. 3	9	No. 4	10	CHANNEL No. 7	11	No. 6	12	No. 7	13
0	0.0000E	0	0.0000E	0	0.0000E	0	0.0000E	0	0.0000E	0	0.0000E	0	0.0000E
1	0.8329E	-5	-0.1014E	-3	0.1985E	-5	-0.9148E	-4	-0.9201E	-5	0.2044E	-4	-0.1629E
2	0.1361E	-4	-0.2080E	-3	-0.2567E	-5	-0.1831E	-3	-0.1419E	-4	0.4474E	-4	-0.3185E
3	0.2542E	-4	-0.3182E	-3	-0.6489E	-5	-0.2811E	-3	-0.3889E	-4	0.8862E	-4	-0.4764E
4	0.3671E	-4	-0.3928E	-3	-0.1182E	-4	-0.3498E	-3	0.7530E	-4	0.1253E	-3	-0.6006E
5	0.4349E	-4	-0.4328E	-3	-0.1356E	-4	-0.3880E	-3	-0.1017E	-3	0.1445E	-3	-0.6929E
6	0.5056E	-4	-0.4671E	-3	-0.1366E	-4	-0.4216E	-3	-0.2695E	-3	0.1675E	-3	-0.7604E
7	0.5608E	-4	-0.5076E	-3	-0.1235E	-4	-0.4582E	-3	-0.5454E	-3	0.1936E	-3	-0.8384E
8	0.6247E	-4	-0.5448E	-3	-0.9782E	-5	-0.4935E	-3	-0.1036E	-2	0.2162E	-3	-0.9063E
9	0.7288E	-4	-0.5833E	-3	-0.7409E	-5	-0.5296E	-3	-0.1884E	-2	0.2426E	-3	-0.1004E
10	0.8373E	-4	-0.6202E	-3	-0.6198E	-5	-0.5677E	-3	-0.2869E	-2	0.2662E	-3	-0.1091E
11	0.9438E	-4	-0.6601E	-3	-0.2324E	-5	-0.6013E	-3	-0.3079E	-2	0.2873E	-3	-0.1168E
12	0.1148E	-3	-0.6911E	-3	0.8232E	-5	-0.6357E	-3	-0.3711E	-2	0.3182E	-3	-0.1260E
13	0.1291E	-3	-0.7241E	-3	0.2073E	-4	-0.6689E	-3	-0.4728E	-2	0.3677E	-3	-0.1349E
14	0.1409E	-3	-0.7434E	-3	0.3007E	-4	-0.6889E	-3	-0.6593E	-2	0.4085E	-3	-0.1422E
15	0.1481E	-3	-0.7619E	-3	0.3947E	-4	-0.7064E	-3	-0.6654E	-2	0.4368E	-3	-0.1461E
16	0.1556E	-3	-0.7792E	-3	0.4857E	-4	-0.7247E	-3	-0.7226E	-2	0.4752E	-3	-0.1510E
17	0.1667E	-3	-0.8046E	-3	0.5772E	-4	-0.7482E	-3	-0.7645E	-2	0.5363E	-3	-0.1600E
18	0.1785E	-3	-0.8224E	-3	0.6707E	-4	-0.7652E	-3	-0.8205E	-2	0.6131E	-3	-0.1656E
19	0.2016E	-3	-0.8608E	-3	0.8925E	-4	-0.8011E	-3	-0.6124E	0	0.7808E	-3	-0.1728E
20	0.2002E	-3	-0.7306E	-3	0.1091E	-3	-0.7129E	-3	0.2592E	-2	0.1038E	-2	-0.1439E
21	0.2062E	-3	-0.7363E	-3	0.8862E	-4	-0.7161E	-3	-0.1314E	-1	0.1719E	-2	-0.1323E
22	0.8858E	-4	-0.2469E	-3	0.8564E	-4	-0.2098E	-3	0.3365E	-2	0.1153E	-2	-0.6945E
23	0.1421E	-3	-0.6056E	-3	0.7200E	-4	-0.5596E	-3	0.3532E	-2	0.1423E	-2	-0.1253E
24	0.1469E	-3	-0.6792E	-3	0.6203E	-4	-0.6331E	-3	0.3554E	-2	0.1468E	-2	-0.1369E
25	0.1578E	-3	-0.7488E	-3	0.6160E	-4	-0.7028E	-3	0.3579E	-2	0.1512E	-2	-0.1482E
26	0.1742E	-3	-0.8255E	-3	0.6697E	-4	-0.7820E	-3	0.3554E	-2	0.1557E	-2	-0.1598E
27	0.1987E	-3	-0.9152E	-3	0.8017E	-4	-0.8698E	-3	0.3504E	-2	0.1603E	-2	-0.1743E
28	0.2036E	-3	-0.9345E	-3	0.8419E	-4	-0.8901E	-3	0.3481E	-2	0.1612E	-2	-0.1769E
29	0.2102E	-3	-0.9520E	-3	0.8859E	-4	-0.9187E	-3	0.3521E	-2	0.1637E	-2	-0.1833E
30	0.2179E	-3	-0.9792E	-3	0.9058E	-4	-0.9462E	-3	0.3514E	-2	0.1653E	-2	-0.1905E
31	0.2213E	-3	-0.1005E	-2	0.9319E	-4	-0.9687E	-3	0.3491E	-2	0.1671E	-2	-0.1952E
32	0.2286E	-3	-0.1031E	-2	0.9488E	-4	-0.9866E	-3	0.3492E	-2	0.1691E	-2	-0.2039E
33	0.2380E	-3	-0.1081E	-2	0.1056E	-3	-0.1017E	-2	0.3545E	-2	0.1733E	-2	-0.2094E
34	0.2427E	-3	-0.1106E	-2	0.9454E	-4	-0.9951E	-3	0.3725E	-2	0.1881E	-2	-0.2032E
35	0.2481E	-3	-0.1130E	-2	0.7901E	-4	-0.9788E	-3	0.3478E	-2	0.2076E	-2	-0.1965E
36	0.2271E	-3	-0.1084E	-2	0.2372E	-4	-0.9111E	-3	0.2637E	-2	0.2711E	-2	-0.1792E
37	0.1833E	-3	-0.1064E	-2	-0.4077E	-4	-0.8482E	-3	-0.1428E	-2	0.3083E	-2	-0.1703E
38	0.1571E	-3	-0.1055E	-2	-0.8518E	-4	-0.8163E	-3	0.2774E	-2	0.3367E	-2	-0.1690E
39	0.3691E	-4	-0.2642E	-3	-0.1242E	-3	-0.3645E	-4	0.3076E	-2	0.2539E	-2	-0.5932E

STRAIN GAGE READINGS

Load No.	CH ¹ CHANNEL	No. 15 21	No. 16 22	No. 17 23	No. 18 24
0		0.0000E 0	0.0000E 0	0.0000E 0	0.0000E 0
1		0.4286E -4	0.1061E -4	0.5128E -4	-0.1641E -3
2		0.8692E -4	0.2673E -4	0.9516E -4	-0.3288E -3
3		0.1406E -3	0.6741E -4	0.1467E -3	-0.5059E -3
4		0.1693E -3	0.1121E -3	0.1760E -3	-0.6378E -3
5		0.1850E -3	0.1330E -3	0.1917E -3	-0.7197E -3
6		0.1972E -3	0.1481E -3	0.2031E -3	-0.7960E -3
7		0.2121E -3	0.1582E -3	0.2188E -3	-0.8814E -3
8		0.2252E -3	0.1663E -3	0.2313E -3	-0.9675E -3
9		0.2405E -3	0.1746E -3	0.2466E -3	-0.1063E -2
10		0.2530E -3	0.1765E -3	0.2581E -3	-0.1163E -2
11		0.2584E -3	0.1394E -3	0.2639E -3	-0.1258E -2
12		0.2702E -3	0.1323E -3	0.2766E -3	-0.1362E -2
13		0.2801E -3	0.1253E -3	0.2870E -3	-0.1466E -2
14		0.2853E -3	0.1236E -3	0.2939E -3	-0.1531E -2
15		0.2903E -3	0.1212E -3	0.3009E -3	-0.1581E -2
16		0.2961E -3	0.1162E -3	0.3077E -3	-0.1637E -2
17		0.3040E -3	0.1146E -3	0.3172E -3	-0.1707E -2
18		0.3103E -3	0.1097E -3	0.3242E -3	-0.1768E -2
19		0.3154E -3	0.9937E -4	0.3312E -3	-0.1829E -2
20		0.2580E -3	0.7685E -4	0.2778E -3	-0.1560E -2
21		0.2263E -3	0.6644E -4	0.2453E -3	-0.1433E -2
22		0.5894E -4	-0.5434E -4	0.9077E -4	-0.7824E -3
23		0.2023E -3	0.2698E -4	0.2237E -3	-0.1368E -2
24		0.2284E -3	0.4406E -4	0.2479E -3	-0.1490E -2
25		0.2512E -3	0.5876E -4	0.2690E -3	-0.1601E -2
26		0.2760E -3	0.7734E -4	0.2913E -3	-0.1721E -2
27		0.3017E -3	0.9471E -4	0.3183E -3	-0.1865E -2
28		0.3076E -3	0.9098E -4	0.3247E -3	-0.1910E -2
29		0.3147E -3	0.8600E -4	0.3310E -3	-0.1962E -2
30		0.3214E -3	0.7724E -4	0.3369E -3	-0.2032E -2
31		0.3270E -3	0.6805E -4	0.3415E -3	-0.2097E -2
32		0.3305E -3	0.6684E -4	0.3444E -3	-0.2176E -2
33		0.3362E -3	0.9974E -4	0.3489E -3	-0.2234E -2
34		0.3216E -3	0.9582E -4	0.3340E -3	-0.2173E -2
35		0.3087E -3	0.8968E -4	0.3206E -3	-0.2122E -2
36		0.2679E -3	0.7076E -4	0.2783E -3	-0.1938E -2
37		0.2451E -3	0.5688E -4	0.2566E -3	-0.1856E -2
38		0.2351E -3	0.5122E -4	0.2481E -3	-0.1822E -2
39		-0.2374E -4	-0.2825E -3	-0.9810E -5	-0.7165E -3

RECENT STRUCTURAL ENGINEERING REPORTS

Department of Civil Engineering

University of Alberta

67. *Inelastic Analysis of Prestressed Concrete Secondary Containments* by D.W. Murray, L. Chitnuyanondh, C. Wong and K.Y. Rijub-Agha, July 1978.
68. *Strength of Variability of Bonded Prestressed Concrete Beams* by D.K. Kikuchi, S.A. Mirza and J.G. MacGregor, August 1978.
69. *Numerical Analysis of General Shells of Revolution Subjected to Arbitrary Loading* by A.M. Shazly, S.H. Simmonds and D.W. Murray, September 1978.
70. *Concrete Masonry Walls* by M. Hatzinikolas, J. Longworth and J. Warwaruk, September 1978.
71. *Experimental Data for Concrete Masonry Walls* by M. Hatzinikolas, J. Longworth and J. Warwaruk, September 1978.
72. *Fatigue Behaviour of Steel Beams with Welded Details* by G.R. Bardell and G.L. Kulak, September 1978.
73. *Double Angle Beam-Column Connections* by R.M. Lasby and Reidar Bjorhovde, April 1979.
74. *An Effective Uniaxial Tensile Stress-Strain Relationship for Prestressed Concrete* by L. Chitnuyanondh, S. Rizkalla, D.W. Murray and J.G. MacGregor, February 1979.
75. *Interaction Diagrams for Reinforced Masonry* by C. Feeg and J. Warwaruk, April 1979.
76. *Effects of Reinforcement Detailing for Concrete Masonry Columns* by C. Feeg, J. Longworth, and J. Warwaruk, May 1979.
77. *Interaction of Concrete Masonry Bearing Walls and Concrete Floor Slabs* by N. Ferguson, J. Longworth and J. Warwaruk, May 1979.
78. *Analysis of Prestressed Concrete Wall Segments* by B.D.P. Koziak and D.W. Murray, June 1979.
79. *Fatigue Strength of Welded Steel Elements* by M.P. Comeau and G.L. Kulak, October 1979.
80. *Leakage Tests of Wall Segments of Reactor Containments* by S.K. Rizkalla, S.H. Simmonds and J.G. MacGregor, October 1979.

81. *Tests of Wall Segments from Reactor Containments* by S.H. Simmonds, S.H. Rizkalla and J.G. MacGregor, October 1979.
82. *Cracking of Reinforced and Prestressed Concrete Wall Segments* by J.G. MacGregor, S.H. Rizkalla and S.H. Simmonds, October 1979.
83. *Inelastic Behavior of Multistory Steel Frames* by M. El Zanaty, D.W. Murray and R. Bjorhovde, April 1980.
84. *Finite Element Programs for Frame Analysis* by M. El Zanaty and D.W. Murray, April 1980.
85. *Test of a Prestressed Concrete Secondary Containment Structure* by J.G. MacGregor, S.H. Simmonds and S.H. Rizkalla, April 1980.
86. *An Inelastic Analysis of the Gentilly-2 Secondary Containment Structure* by D.W. Murray, C. Wong, S.H. Simmonds and J.G. MacGregor, April 1980.
87. *Nonlinear Analysis of Axisymmetric Reinforced Concrete Structures* by A.A. Elwi and D.W. Murray, May 1980.
88. *Behavior of Prestressed Concrete Containment Structures - A Summary of Findings* by J.G. MacGregor, D.W. Murray, S.H. Simmonds, April 1980.
89. *Deflection of Composite Beams at Service Load* by L. Samantaraya and J. Longworth, June 1980.
90. *Analysis and Design of Stub-Girders* by T.J.E. Zimmerman and R. Bjorhovde; August 1980.
91. *An Investigation of Reinforced Concrete Block Masonry Columns* by G.R. Sturgeon, J. Longworth and J. Warwaruk, September 1980.
92. *An Investigation of Concrete Masonry Wall and Concrete Slab Interaction* by R.M. Pacholok, J. Warwaruk, and J. Longworth, October 1980.
93. *FEPARCS5 - A Finite Element Program for the Analysis of Axisymmetric Reinforced Concrete Structures - Users Manual* by A. Elwi and D.W. Murray, November 1980.
94. *Plastic Design of Reinforced Concrete Slabs* by D.M. Rogowsky and S.H. Simmonds, November 1980.
95. *Local Buckling of W Shaped Used as Columns, Beams, and Beam-Columns* by J.L. Dawe and G.L. Kulak, March 1981.
96. *Dynamic Response of Bridge Piers to Ice Forces*, by E.W. Gordon and C.J. Montgomery, May 1981.
97. *Full-Scale Test of a Composite Truss*, by Reidar Bjorhovde, June 1981.